K^+−Ribosome Interactions Determine the Large Enhancements of ^{39}K NMR Transverse Relaxation Rates in the Cytoplasm of *Escherichia coli* K-12†

Harry J. Guttman,‡ Scott Cayley,§ Man Li,§ Charles F. Anderson,‡ and M. Thomas Record, Jr.*,‡,§

Departments of Chemistry and Biochemistry, University of Wisconsin—Madison, Madison, Wisconsin 53706

Received October 3, 1994; Revised Manuscript Received November 18, 1994®

ABSTRACT: As a probe of physical chemical properties of the intracellular environment, we measured ^{39}K NMR transverse relaxation rates in concentrated cell slurries of *Escherichia coli* K-12 grown in minimal medium over a range of osmolarities (from 0.1 to 1.0 OsM) and after plasmolysis. The ^{39}K transverse relaxation at a resonance frequency of ~18.67 MHz is biexponential under all conditions, and 100% of the expected signal intensity is detected. Both components of the ^{39}K NMR transverse relaxation are very fast, and the difference between the fast and slow relaxation rates is very large compared to previous measurements on ^{23}Na and ^{39}K in protein and nucleic acid solutions *in vitro*. The ^{39}K transverse relaxation rates decrease as the osmolarity of the growth media increases but increase dramatically when cells grown in 0.1 OsM media are plasmolyzed at 1.0 OsM. The homogeneous nature and the 100% visibility of the ^{39}K signal indicate the existence of fast exchange among the multiple, magnetically distinguishable populations of ^{39}K which probably exist in the cytoplasm. The absence of static quadrupolar splitting of the cytoplasmic ^{39}K signal (as indicated by a single peak in the spectrum) indicates that the cytoplasm, as probed by ^{39}K NMR, behaves like a concentrated but isotropic nucleic acid solution rather than an anisotropic nucleic acid liquid crystal. To understand the origins of the striking NMR relaxation behavior of ^{39}K in viable cells, we have investigated NMR transverse relaxation rates of ^{39}K (and also ^{23}Na and ^{35}Cl) in *E. coli* 50S and 70S ribosome solutions *in vitro*. At concentrations of ions and of ribosomes that to the extent possible mimic those of the cytoplasm of *E. coli*, we find that ^{39}K, ^{23}Na, and ^{35}Cl transverse relaxation rates all exhibit biexponential behavior, and ^{39}K and ^{23}Na exhibit the large magnitudes and the large difference between the slow and the fast relaxation rates observed in viable cells. These polyanionic ribosome solutions are the only *in vitro* model system discovered to date that exhibits ^{39}K transverse relaxation rates comparable to those in viable cells. We conclude that K^+−ribosome interactions are the dominant source of the NMR properties of K^+ in *E. coli*. We propose that the relatively small dependence of *in vivo* ^{39}K transverse relaxation rates in the cytoplasm of *E. coli* on cytoplasmic K^+ concentration (increased by increasing the osmolarity of the growth medium) results from near-compensation between two significant contributions: (1) the ratio of K^+-to-nucleic acid phosphate increases, tending to decrease the ^{39}K transverse relaxation rates, and (2) the concentration of ribosomal particles increases because the volume of cytoplasmic water decreases, tending to increase the ^{39}K transverse relaxation rate. We propose that the dramatic increase observed in the ^{39}K transverse relaxation rates in plasmolyzed cells results from the increase in cytoplasmic ribosome concentration at constant K^+: phosphate ratio and the large decrease in cytoplasmic water upon plasmolysis.

NMR spectroscopy, a noninvasive method of investigating intracellular environments, has been applied to monitor ion concentrations and ion fluxes in many systems including *Escherichia coli* (Castle et al., 1986a,b; Richey et al., 1987; Shacher-Hill & Shulman, 1992), halobacteria (Shporer & Civan, 1977), yeast (Ogino et al., 1983; Rooney & Springer, 1991), red blood cells (Ogino et al., 1985; Shinar & Navon, 1991), rat heart (Foy & Burstein, 1990; Hirasihi et al., 1990; Seo et al., 1990), and rat salivary gland (Seo et al., 1993; Steward et al., 1991). The transverse relaxation properties of spin $^3/_2$ cationic quadrupolar nuclei (^{23}Na, ^{39}K, and ^{87}Rb) in the viable cells (i.e., cells capable of propagation) used in most of these studies have three characteristics: (1) the functional form of the transverse relaxation is biexponential at magnetic fields above 7.5 Tesla; (2) the magnitudes of both of the transverse relaxation rates are large; and (3) the differences between the two are large compared to those in all biopolymer solutions investigated previously. For *in vitro* solutions of proteins or nucleic acids with physiologically relevant viscosity (~1.5 times that of pure water; Lewis et al., 1990) and macromolecular concentrations (~275−420 mg/mL; Cayley et al., 1991), NMR relaxation rates of spin $^3/_2$ quadrupolar cations (e.g., Braunlin & Nordenskiöld, 1984; Seo et al., 1993; van Dijk et al., 1987) are rarely detected as biexponential and have relaxation rates that are much smaller than those in viable cells. By the three criteria above,

† This work was supported by a grant from the NIH (GM47022). H.J.G. is grateful for support from a graduate training grant in Molecular Biophysics (NIH GM08293) between June 1991 and June 1994. The NMR experiments were performed at National Magnetic Resonance Facility at Madison. This facility is supported by NIH (RR02301) and equipment was purchased with funds from UW NSF (DMB-8415048), NIH (RR02301, RR01201, RR02781), and the U.S. Department of Agriculture.

* Author to whom correspondence should be addressed at Department of Biochemistry, 420 Henry Mall, Madison, WI 53706. Phone: (608) 262-5332, Fax: (608) 262-3453, E-mail: Record@chem.wisc.edu.

‡ Department of Chemistry.

§ Department of Biochemistry.

® Abstract published in *Advance ACS Abstracts,* January 1, 1995.

0006-2960/95/0434-1393$09.00/0

Table 1: Motional Regimes for Spin $^3/_2$ NMR Relaxation in the Motional Narrowing Limit[a]

motional regime	$\omega_L\tau_{slowest}$	decay functional form	relative values of relaxation rates
extreme motional narrowing[b]	$\ll 1$	single exponential	$R_2 = R_1$
near-extreme motional narrowing	$\lesssim 1.5$	single exponential	$R_2 > R_1$
slow motional narrowing[c]	$\gtrsim 1.5$	double exponential	$R_{2f} > R_{1f}$ $R_{2s} > R_{1s}$

[a] Descriptions in this table are general guidelines assuming adequate signal-to-noise; see text. [b] Equivalent to type d spectra as designated by Rooney et al. (1988). [c] Equivalent to type c spectra as designated by Rooney et al. (1988).

previous measurements of NMR relaxation rates of quadrupolar cations in physiologically relevant *in vitro* solutions have not been able to mimic the intracellular environment of a viable cell. Before the present study, neither the molecular species with which these cations interact nor the character of the interactions that cause large transverse relaxation rates of ^{39}K and ^{23}Na in viable cells were known.

To understand better the physical chemical nature of the intracellular environment, we monitor the transverse relaxation of ^{39}K, the osmotically regulated solute primarily responsible for osmotic pressure of the cytoplasm of *E. coli*, as a function of osmolarity of the growth medium, and during a titration with NaCl to high osmolarity under nongrowing conditions (plasmolysis). From our analysis of literature data on quadrupolar NMR relaxation and our multinuclear (^{23}Na, ^{35}Cl, and ^{39}K) measurements of *in vitro* ribosome solutions, which we propose are an appropriate model for the *in vivo* environment of K^+, we infer the nature of the cytoplasmic environment in *E. coli*, as sensed by the quadrupolar ^{39}K NMR transverse relaxation and consider the nature of the NMR relaxation of quadrupolar nuclei in viable cells.

BACKGROUND

NMR Terminology. The NMR signal [either the free induction decay (FID) or Fourier-transformed (FT) spectrum] may be described as homogeneous or heterogeneous (Fukushima & Roeder, 1981). A *homogeneous* signal results from either a single population of nuclei or multiple populations of nuclei (i.e., magnetically distinct environments) in fast exchange, where all environments are sampled on a time scale much more rapid than the fastest NMR relaxation rate, so that the signal is a population-weighted average of these environments. With a single population or multiple populations, homogeneity implies that every nucleus makes an equivalent contribution to the NMR signal (in the sense that it experiences all of the magnetically distinguishable environments on the NMR time scale), and therefore the NMR signal can be represented by a single time correlation function. A *heterogeneous* signal is a composite of individually homogeneous signals. The present discussion pertains to a homogeneous signal except where noted.

Four motional regimes of the processes that contribute to NMR relaxation can be distinguished (see Table 1) (Forsén & Lindman, 1981; Rooney et al., 1988). The motional regimes are a primary determinant of the functional form of the frequency dependence of the relaxation rates of a given nucleus. *Extreme motional narrowing* (e.g., ^{23}Na in a NaCl solution) describes the motional regime where the longitudinal and transverse relaxation functional forms are independent of the Larmor frequency (ω_L), are well-approximated by a single-exponential decay, and therefore have equal NMR relaxation rates (i.e., $\tau_c\omega_L \ll 1.0$, where τ_c is the correlation time for the slowest motional process that contributes to NMR relaxation). *Near-extreme motional narrowing* (e.g., ^{23}Na in a DNA solution where [Na]/[P] = 1 and $\omega_L > 90$ MHz) is defined as the motional regime where the longitudinal and transverse relaxation functional forms are well-approximated by a single-exponential decay, but the NMR relaxation rates are not equal (typically, $\tau_c\omega_L < 1.5$ for spin $^3/_2$ nuclei; Bull, 1972; Halle & Wennerström, 1981). The motional regime that applies most often to transverse relaxation of cations *in vivo* is that which we define as the *slow motional narrowing* regime. For a spin $^3/_2$ signal in this regime, the functional forms describing the transverse and longitudinal relaxation are biexponential. The fast (f) and slow (s) components of the transverse (2) and longitudinal (1) relaxation rates are designated R_{2f}, R_{2s}, R_{1f}, and R_{1s}, respectively. The *slow motion* regime occurs when the mean electric field gradient is nonzero (on the relevant time scale), resulting in first-order quadrupolar splitting (also termed static quadrupolar splitting). In the slow motion regime for a spin $^3/_2$ nucleus the FT spectrum consists of either three peaks, whose separation is proportional to the extent of static quadrupolar splitting (if the angle between the direction of the mean electrostatic field gradient and the direction of the applied magnetic field is single-valued, or nearly so), or a powder pattern, if this angle is randomly distributed. [For a review of quadrupolar nuclei see Forsén and Lindman, (1981).] Quadrupolar NMR studies of anisotropic samples (such as liquid crystals) typically yield signals that are in the slow motion limit, while studies of isotropic systems usually exhibit behavior in the motional narrowing regime.

From the perspective of experiment and data analysis, the applicability of the designation of motional regimes may depend on the quality of the data. For example, if signal-to-noise were infinite the longitudinal and transverse NMR relaxation of spin $^3/_2$ nuclei would be detectably biexponential, for any finite (nonzero) value of $\tau_c\omega_L$. Conversely, if signal-to-noise is too low, neither biexponential relaxation nor the differences between longitudinal and transverse relaxation rates can be observed even when $\tau_c\omega_L > 1.5$.

For a signal in the slow motional narrowing regime, the NMR longitudinal and transverse relaxation of spin $^3/_2$ nuclei is biexponential (Hubbard, 1970). The ratio of the pre-exponential factors (referred to here as amplitudes) of the two NMR transverse relaxation rates (slow:fast) is always 2:3. Observation of a single-exponential transverse relaxation comprising 40% of the expected signal intensity typically results from the inability to detect the fast transverse relaxation component, because of its rapid decay rate (cf. Springer, 1987). The phenomenon of NMR "invisibility" depends not exclusively on the physical properties of the system but also (in general) on the technical capabilities of

the probe and spectrometer.

Two-State NMR Model for Cation−DNA Interactions. In a polymeric DNA solution, the various transverse or longitudinal relaxation rates of a quadrupolar monovalent cation, M^+ (e.g., ^{23}Na or ^{39}K), typically can be fitted to a two-state model to describe the ion distribution, as probed by NMR (Anderson & Record, 1990; Braunlin & Nordenskiöld, 1984). In this model, the observed NMR signal is homogeneous with a relaxation rate (R_{obs}) which is a population-weighted average of contributions from nuclei in the vicinity of and therefore affected by the DNA (designated as B, bound) with the characteristic relaxation rate R_B, and nuclei with relaxation rate R_F that do not experience the DNA (designated as F, free) (Anderson & Record, 1990). Exchange of nuclei between these two NMR states is much more rapid than R_B (or R_F).

$$R_{obs} = p_F R_F + p_B R_B = R_F + (R_B - R_F) r^o [P]/[M^+] \quad (1)$$

where p_F and p_B are the fraction of cations in the free and bound state, respectively ($p_F + p_B = 1$), $r^o \equiv [M^+]_B/[P]$, and $[M^+]$ and [P] are total concentrations of cation and DNA phosphate. For polymeric DNA, R_{obs} is found experimentally to be linear in the ratio $[P]/[M^+]$. This linearity implies that the composite quantity $(R_B - R_F)r^o$ is constant. The intercept of this line, R_F, is approximately equal to or slightly larger than the relaxation rate of the cation in a salt solution of comparable concentration in the absence of DNA (Stein et al., 1995). At a given [P], the maximum relaxation rate of a rapidly exchanging cation in a DNA solution is observed under salt-free conditions where $[P]/[M^+]$ is unity (Stein et al., 1995). Alternatively, when $[P]/[M^+]$ is much less than unity (i.e., in a large excess of salt), R_{obs} approaches its minimal possible value, R_F.

MATERIALS AND METHODS

E. coli Cell Preparation. E. coli K-12 strain MG1655 was grown aerobically at 37 °C in MOPS-buffered glucose minimal medium (MBM; 0.1 OsM; Cayley et al., 1989) or in a very low osmolarity (0.027 OsM) medium (VLOM) containing 10 mM MOPS, 8.2 mM NH_4OH, 4.4 mM glucose, 0.5 mM $MgSO_4$, 0.5 mM KH_2PO_4, and 10 μM $FeSO_4$ (D. Cayley, M. W. Capp, H. J. Guttman, and M. T. Record, Jr., unpublished data). For MBM, NaCl was added to adjust the external osmolarity. The external osmolarity was determined with a Wescor vapor phase osmometer. Three liters of media were inoculated with ≤3 mL of a saturated cell culture, grown to mid-log phase (~4×10^8 cell/mL), and harvested by centrifugation for 8 min at 8700*g* at room temperature. To remove extracytoplasmic K^+, cell pellets were suspended in 250 mL of iso-osmotic wash buffer (WB is composed of growth media except that glucose and K^+ are replaced by an iso-osmotic amount of NaCl), recentrifuged, and resuspended in WB to give the dense cell slurry used for the NMR experiments. The dry weight of the cell slurries was determined as described in Cayley et al. (1991) and was in the range of 160−200 mg dry weight/mL.

To prepare plasmolyzed cell samples, cells grown in MBM were harvested as above except that the wash buffer contained 0.5 M NaCl (1.02 OsM). Plasmolysis removes water from the cytoplasm, causing a reduction in cytoplasmic volume. Under our plasmolysis conditions, no change in the amount of any detectable cytoplasmic solute occurs upon plasmolysis (Cayley et al., 1991). Hence in our plasmolyzed cells the total concentrations of all solutes increase by the same factor (3-fold), due to the reduction in the amount of cytoplasmic water.

For both plasmolyzed cells (1.0 OsM) and cells grown at high osmolarity (0.6 OsM, 1.0 OsM), ^{39}K transverse relaxation rates decrease significantly as a function of time after harvest (data not shown). The kinetics appear first order with a half-life of ~15 h. No such time dependence was observed in low-osmolarity cells.

The relaxation data for the cell samples reported in Figure 2 are the first point from the time course which was always less than 3 h from the start of the harvest procedure to the middle of the time of the data acquisition. (The physiological basis of this time dependence, which is not accompanied by a concomitant loss in viability and does not appear to be leakage of K^+ to the extracellular environment, is currently being investigated.)

Ribosome Samples. Frozen samples of 50S and 70S *E. coli* ribosomes were obtained from Dr. Peter Moore of Yale University. 50S ribosomes had been stored at −80°C at a ribosome concentration of 35 mg/mL in 10 mM Tris, 10 mM magnesium acetate, 60 mM NH_4Cl, and 6 mM β-mercaptoethanol at pH 7.6. Salt and buffer concentrations in the 50S ribosome solution were changed by dialysis. We extensively dialyzed at 4 °C (five 12 h periods using 12−14 kDa cutoff) against a solution containing 7 mM $MgSO_4$, 46 mM KGlu, and 0.9 mM MOPS at pH 7.6, lyophilized to dryness, and rehydrated to desired NMR solution conditions by addition of salts if necessary.

70S ribosomes had been stored at −80 °C at a concentration of 84 mg/mL with 20 mM Tris, 10 mM magnesium acetate, 0.1 mM EDTA, and 100 mM NH_4Cl at pH 7.5. After thawing, 70S ribosome samples were centrifuged at 7000*g* for 7 min. Salt and buffer concentrations in the 70S ribosome solution were changed by extensive dialysis at 4 °C (five 12 h periods using 12−14 kDa cutoff) against a solution containing 5 mM $MgSO_4$, 46 mM KGlu, and 1 mM MOPS at pH 7.6 or against a solution containing 40 mM NaCl, 4.7 mM $MgCl_2$, and 1.0 mM MOPS at pH 7.6. After dialysis, the solution was diluted and/or salts were added to attain desired NMR solution conditions.

The ribosome concentration was determined by absorbance at 260 nm using an extinction coefficient of 16 mL mg^{-1} cm^{-1} which corresponds to an A_{260} of 1.0 (Wishnia et al., 1975). Final cation concentrations were determined analytically (see below).

BSA Preparation. BSA was purchased from Sigma (A6918). Salts were removed by dialysis at 4 °C against deionized water (conductance 18.1 MΩ). After dialysis, the BSA solution was freeze-dried. Samples were made by adding dry BSA to the salt solution and then shaking the tubes in an Erlenmeyer flask in an air shaker at 37 °C until samples were fully dissolved (typically 12−48 h). BSA concentrations were determined from the absorbance at 278 nm using an extinction coefficient of 0.66 mL mg^{-1} cm^{-1} (Noelken & Timasheff, 1967).

NMR Spectroscopy. NMR data were collected on a Bruker AM-400 (9.395 Tesla) wide-bore multinuclear spectrometer using a 10 mm BB probe tuned to 18.67 MHz for ^{39}K, 105.85 MHz for ^{23}Na, and 39.21 MHz for ^{35}Cl. Data collection

parameters were optimized for analysis of the free induction decay (FID).

For ^{39}K experiments on cell samples, the FID consisted of 4096 points with no zero filling. The sweep width was 125 kHz. The delay to acquisition of the first point for each scan was at least 280 μs and was typically set to 380 μs to minimize acoustic ringing in the signal. With the relaxation delay set to zero the acquisition time was ~0.016 s (at least 10 times R_{2s} in these samples). For all the other samples, there was no zero filling, the relaxation delay was set to zero, the FID typically consisted of 8192 points, and the acquisition time was at least 8 (usually 10) times R_{2s}. The delay to acquisition of the first point for each scan was at least 280 μs.

For all ^{39}K experiments, the 90° pulse width was 45 μs and was not significantly dependent on solution conditions. ^{23}Na and ^{35}Cl 90° pulse widths were measured for each sample and were typically on the order of 19 and 27 μs, respectively.

For the ^{39}K experiments, shimming was performed on a standard containing ~1 M KCl in 100% D_2O, after which samples of interest were placed in the spectrometer and temperature-equilibrated for at least 15 min. The ^{39}K R_2 of the shimming standard, from line width determinations using Bruker software data analysis, was always less than 0.022 ± 0.001 ms^{-1}. Inverse recovery measurements of the longitudinal relaxation rate of the shimming standard give an R_1 = 0.021 ± 0.001 ms^{-1}. This crude method of shimming is sufficient since we obtain values of R_2 for all KCl standards which are ≤0.019 ± 0.001 ms^{-1} and values of R_1 (from inverse recovery measurements and data analysis using Bruker software) of 0.017 ± 0.001 ms^{-1}. Thus, inadequate shimming resulted in an increase of no more than 0.002 ms^{-1} in the R_2 of KCl. This increase is negligible compared to the magnitudes of the transverse relaxation rates measured here.

For the ^{23}Na and the ^{35}Cl experiments, either 10% D_2O was added (as indicated) or a 100% D_2O-NaCl shimming standard was used to shim the magnet as in the KCl shimming method above. (^{23}Na is more sensitive to inadequate shimming than are ^{35}Cl and ^{39}K.) ^{23}Na transverse relaxation rates in NaCl solutions using the NaCl−D_2O shimming standard were typically 0.021 ms^{-1}, comparable to 0.018 ms^{-1} expected for ^{23}Na in a NaCl solution. Again, this increase is negligible compared to the transverse relaxation rates measured here.

All NMR experiments were performed at a temperature of 296 ± 1 K. Using a platinum thermistor to measure the temperature before and after 15 min of NMR scanning on a cell slurry, we detected no sample heating.

NMR Data Analysis and General Method of Functional Form Determination. When the transverse relaxation rates are fast compared to the effective increase in the transverse relaxation rates due to magnetic inhomogeneity in the sample, accurate determinations of transverse relaxation rates can be obtained using single pulse (90°) experiments because a large number of points can be used to define the signal. The large number of points, the large difference between R_{2f} and R_{2s} (greater than a factor of 5 in most cases here), and the large weight of the fast transverse relaxation component (60%) all facilitate the accurate decomposition of R_{2f} and R_{2s} from the signal of a single pulse experiment. Therefore, to obtain transverse relaxation rates, we fitted the FIDs directly.

The real and imaginary components of the FIDs were transferred in binary format to a VAXstation 3100 and converted to ascii format for fitting and plotting. Data points resulting from acoustic ringing in the probe head were removed from the data set prior to the fitting procedure.

The real and imaginary components of the FID were fitted using the following functional forms:

$$I_{\text{real}}(t) = A[\alpha e^{-R_{2s}t}\cos(\omega t + \theta_s) + (1-\alpha)e^{-R_{2f}t}\cos((\omega+\Delta\omega)t + \theta_f)] \quad (2a)$$

$$I_{\text{imaginary}}(t) = A[\alpha e^{-R_{2s}t}\sin(\omega t + \theta_s) + (1-\alpha)e^{-R_{2f}t}\sin((\omega+\Delta\omega)t + \theta_f)] \quad (2b)$$

where t is time, A is the amplitude (proportional to the concentration of the measured nucleus), α is the fraction of the amplitude from the slow component, R_{2s} and R_{2f} are the slow and fast transverse relaxation rates, ω and $(\omega + \Delta\omega)$ are the frequencies of slow and fast component (where $\Delta\omega$ is the dynamic frequency shift; Fouques & Werbelow, 1979; Werbelow, 1979; Werbelow & Marshall, 1981), and θ_s and θ_f are the phases of the slow and fast components. Both real and imaginary components of the FID are fitted simultaneously using NONLIN (Johnson & Frasier, 1985; Straume et al., 1991).

We analyze the FID rather than the spectrum to obtain the transverse relaxation rates, because analysis of the FID implicitly accounts for the dead time after the 90° pulse and before the commencement of data acquisition. This is important because the pre-exponential factor of the exponential part of the FID (A, the amplitude, in eq 2) is proportional to the concentration of the NMR-detected species in the sample. As long as one knows the absolute value of the time with respect to the middle of the 90° pulse (i.e., when $t = 0$), the exponential functional form does not lose information about the true value (i.e., zero-time value) of the amplitude even if a data point is not measured explicitly at zero time. However if the FID is Fourier transformed, the functional form of the resulting spectrum (a Lorentzian or sum of Lorentzians) must be modified (and therefore the complexity of the function form increased) to account for the dead time in order to evaluate the amplitude correctly. The conventional method of numerical integration of the spectrum to obtain the amplitude is not adequate for our analyses, because the "raw-data" spectrum inherently loses the zero time information upon transforming the FID (i.e., using conventional FFT methods employed by most spectrometers).

All data were first fitted to a single-exponential decay by fixing α at unity and floating A, R_{2s}, ω, and θ_s; $\Delta\omega$ was fixed at zero and θ_f was set equal to θ_s. If systematic differences were observed between the single-exponential fitting and the data (as determined by visual comparison of the fitted curve with the data or by inspection of the residuals produced by NONLIN), a double-exponential fitting was performed by floating A, R_{2s}, R_{2f}, θ_s, and ω. In this fitting step, α was fixed at 0.4, $\Delta\omega$ was fixed at zero, and θ_f was set equal to θ_s. Any systematic differences between the latter fitting and the data were attributed to a dynamic frequency shift ($\Delta\omega$). In this situation, another fitting was obtained by floating A, R_{2s}, R_{2f}, θ_s, ω, and $\Delta\omega$; α was fixed at 0.4, and θ_f was set equal to θ_s. Setting $\theta_f = \theta_s$ assumes that the

phase difference between the two peaks is the same (i.e., the first-order phase correction is zero). This appears to be a very good assumption considering the small difference in the chemical shift (due to the dynamic frequency shift) between the two peaks.

In the double-exponential fittings, if α was floated, its best fitted value was always equal to 0.4 within error (estimated absolute errors, 1 SD, in α are typically ~0.05−0.1), and the relaxation rates were the same within error as those obtained with α fixed at 0.4. However, when α was floated, the correlations between α and other parameters (e.g., R_{2f}, R_{2s}, or A) were very high (typically higher than 0.96), implying large uncertainties in the correlated parameters.

When signal-to-noise was good in the samples having large transverse relaxation rates (usually ^{23}Na, sometimes ^{35}Cl, and rarely ^{39}K), floating the dynamic frequency shift ($\Delta\omega$) gave better fittings than when $\Delta\omega$ was fixed to zero. However, there was typically a large error in its determination (estimated relative errors, 1 SD, in $\Delta\omega$ are ~30−50%), and therefore we do not have confidence in its value. The transverse relaxation rates obtained are the same within error for the fittings of a given data set whether $\Delta\omega$ was fixed at zero or floated.

NMR Determination of Ion Concentrations Using Standards. Since the amplitude (A in eq 2) of the FID is proportional to the detectable ("visible") amount of that ion in a sample, determination of these amounts was performed by comparison of the fitted amplitude of a standard with the fitted amplitude of the sample of interest. The standards were volumetrically prepared salt solutions at approximately the same concentrations as those in the samples of interest. The standards were prepared so that the concentrations were known to within 1% accuracy.

Analytical Determinations of Cation Concentration. For the ribosome solutions, cation concentrations were determined after dialysis to account for the redistribution of the ions across the membrane that occurs when polyelectrolytes are dialyzed against salt solutions (i.e., the Donnan effect). Mg^{2+} concentration was determined by ICPES (inductively coupled plasma emission spectroscopy using a Leeman Lab Inc. plasma spectrometer ICP 2.5 source coupled to a Minuteman 0.5 m monochrometer and using a 1P28 photomultiplier tube for detection) at a wavelength of 287.6 nm; the concentration range between 2 and 10 ppm was linear with peak height. Mg^{2+} concentrations were calibrated to Mg^{2+} standard solutions (Sigma) or analytically prepared $MgCl_2$ and $MgSO_4$ solutions. K^+ concentration was determined by FES (flame emission spectroscopy) using a Heath McPherson FES at 766.49 nm; the linear range was determined to be 10−50 ppm. Na^+ concentration was determined by FES at 589.0 nm; the linear range was 5−20 ppm. K^+ and Na^+ standards were prepared analytically from chloride salts. The solutions for which ion concentrations were measured were diluted to obtain K^+, Na^+, or Mg^{2+} concentrations within the linear concentration range of the respective standard curves. Each sample was scanned at least three times to obtain a mean value of the absorbance.

For the cell slurries, the potassium concentration was determined using dry weight determinations or estimations thereof [see Richey et al. (1987) or Cayley et al. (1991)]. The determinations of the potassium concentration in the cell slurries had ~10% relative error (1 SD) (Cayley et al., 1991).

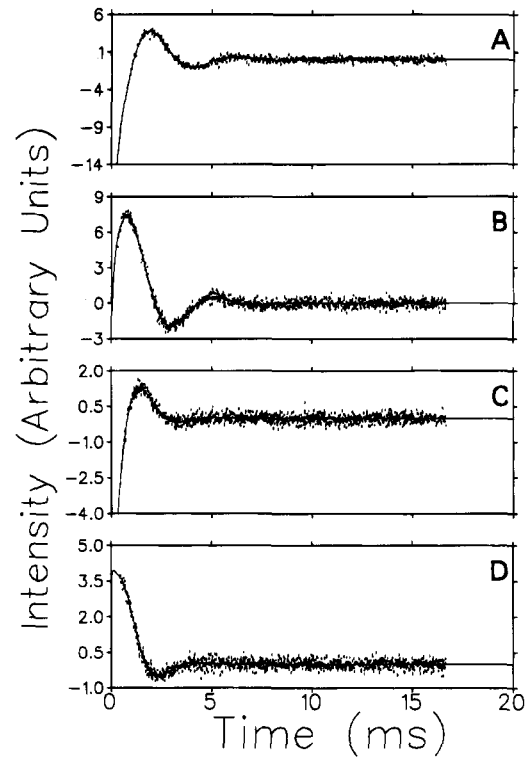

FIGURE 1: FIDs of *E. coli* cell slurries. Real (A) and imaginary (B) components of the FID of a 1.0 OsM cell slurry. Real (C) and imaginary (D) components of the FID of a plasmolyzed cell slurry at 1.0 OsM. The dotted lines show data and solid lines show double-exponential fittings.

RESULTS

We Observe 100% of the Expected Signal When ^{39}K Free Induction Decays in E. coli Cells Are Fitted with a Double-Exponential Decay. Figure 1 shows representative data and fittings of the real and imaginary components of the FID of ^{39}K in cell slurries. In Figure 2, ^{39}K transverse relaxation rates of *E. coli* cell slurries (obtained from analysis of the FID using eq 2 as described in Materials and Methods) are plotted as a function of the osmolarity of the growth medium. Within experimental error (1 SD is ~15% absolute error), we observe 100% of the expected signal for all cell samples. All samples exhibit biexponential relaxation. The relaxation rates R_{2s} and R_{2f} are very large compared to a solution of KGlu (greater than a factor of 25 and 250, respectively), and the difference between R_{2s} and R_{2f} is also very large (between 5 and 10 ms^{-1}).

Slurries prepared from cells grown at low osmolarities (0.027 and 0.1 OsM) contain less K^+ than those grown at higher osmolarities, reducing signal-to-noise and resulting in larger errors for the fast relaxation rates. Because of low signal-to-noise in these low osmolarity cell samples, there was no significant difference in the quality of the fittings between the single and double exponential. However, the ratios of the total amplitudes from the single- and double-exponential fittings were always 2:5, indicating that 60% of the signal is lost in the single-exponential fitting compared to the double-exponential fitting. Also, the high quality of the fittings of the 0.6 and 1.0 OsM data to the double-exponential time decay further validates the applicability of this functional form for ^{39}K NMR in the slurries with low $[K^+]$.

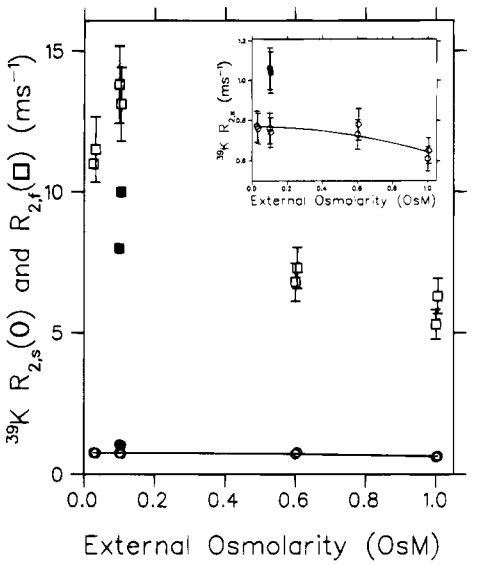

FIGURE 2: ^{39}K transverse relaxation rates in *E. coli* K-12 as a function of osmolarity of the growth medium. Transverse relaxation rates [R_{2f} (□) and R_{2s} (○)] of ^{39}K in *E. coli* cell slurries are plotted as a function of the osmolarity of the growth medium. Open squares are ^{39}K relaxation rates of cells grown, washed, and concentrated with WB at the indicated osmolarities. Solid squares are ^{39}K relaxation rates of slurries of plasmolyzed cells. Three of the R_{2f} points do not have error bars due to low signal-to-noise. Therefore these three points represent semiquantitative estimates of R_{2f}.

When the data from any cell sample are fitted using the single-exponential functional form, the amplitudes are ~40% of that obtained from the double-exponential fittings. This suggests that poorer signal-to-noise would make the fast component undetectable and would yield the 40% NMR visibility that is frequently observed in *E. coli* and yeast (e.g., Castle et al., 1986a).

The Absence of Quadrupolar Splitting Implies a Homogeneous Character of ^{39}K Relaxation in the Cytoplasm of E. coli. To demonstrate the absence of significant static quadrupolar splitting in the NMR signal of ^{39}K in *E. coli*, we display the absorptive components of the Fourier transform of the FIDs of *E. coli* cells grown at 1.0 OsM growth media and cells grown at 0.1 OsM and plasmolyzed at 1.0 OsM (Figure 3A,B). These two samples have the highest concentrations of nucleic acid phosphate of the samples we examined and are therefore the most likely to manifest any static quadrupolar splitting of the ^{39}K signal that could be due to slow motions associated with potassium−nucleic acid interactions. However, these two spectra (and all others) show only a single peak in the spectrum and therefore give no evidence of any static quadrupolar splitting of the ^{39}K signal. In principle, multiple-quantum NMR spectroscopy could more firmly establish the isotropic and homogeneous nature of the signal, but the signal-to-noise of a typical cell slurry would not be sufficient for multiple-quantum experiments of accuracy comparable to that of the single pulse experiment. Also, the time dependence of the relaxation rates observed for high osmolarity and plasmolyzed cell slurries (see Materials and Methods) would limit the duration and hence the reliability of a multiple-quantum experiment.

K^+−Ribosome Interactions Cause the Magnitudes and the Difference between the Transverse Relaxation Rates of ^{39}K in vitro. The bulk of nucleic acid phosphate in the cytoplasm of *E. coli* is in the form of ribosomal RNA (ribosomal

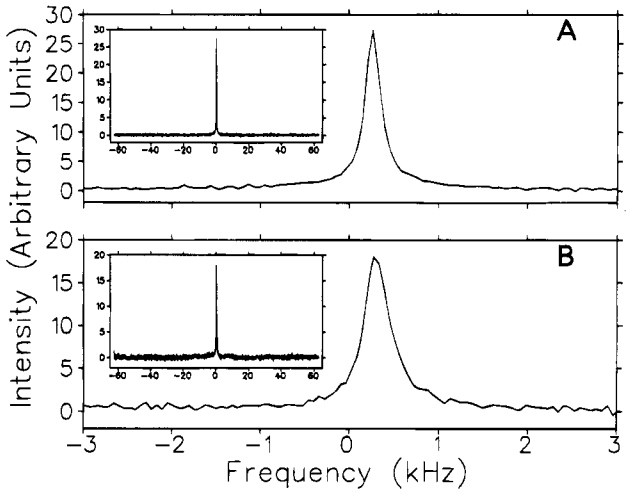

FIGURE 3: Spectra of *E. coli* cell slurries. Absorptive components of spectra of a 1.0 OsM cell slurry (A) and of a plasmolyzed cell slurry (B). The Fourier transforms were performed using FELIX with no zero filling or line broadening. The absorptive components of the Fourier transformed FIDs correspond to the FIDs shown in Figure 1.

Table 2: ^{39}K Transverse Relaxation Rates

system	R_2 or R_{2s}, R_{2f} (ms^{-1})	visibility (%)[e]
E. coli[a,b] (1.0 OsM)	0.63 ± 0.06 5.8 ± 0.5	98 ± 15
70S ribosomes[a,c]	0.37 ± 0.04 5.6 ± 0.6	96 ± 10
50S ribosome subunits[a,c]	0.47 ± 0.05 6.3 ± 0.6	98 ± 10
K-DNA[d] (extrapolated 1:1 [M^+]:[P])	0.38 ± 0.03	(100)
1 mM KGlu in 470 mg/mL BSA[a]	0.099 ± 0.005	97 ± 10
0.75 M KGlu[a]	0.028 ± 0.003	(100)

[a] T = 296 K; ω_L = 18.672 MHz. [b] [nucleic acid phosphate] = 0.43 M, [K^+] = 0.55 M, [Mg^{2+}] = 0.09 M. Glutamate is the most abundant nonpolymeric cytoplasmic anion. [c] For 70S: [ribosomal phosphate] = 35.5 mM, $[K^+]_{total}$ = 56.0 mM, $[Cl^-]_{total}$ = 10.0 mM (10 mM KCl was added to the 70S ribosome solution after dialysis), $[Mg^{2+}]_{total}$ = 14.0 mM, [NaN_3] = 5.0 mM, [MOPS] = 0.5 mM, [β-mercaptoethanol] = 3 mM, pH 7.6. For 50S: [ribosomal phosphate] = 119.6 mM, $[K^+]_{total}$ = 195.0 mM, $[Mg^{2+}]_{total}$ = 45.5 mM, [MOPS] = 5.6 mM. [d] Braunlin and Nordenskiöld (1984); T = 297 K, ω_L=16.68 MHz. [e] Percent visibility is 100 times the ratio of the observed NMR signal intensity to the expected NMR signal intensity from analytical determinations. (100) means that 100% visibility is assumed.

phosphate concentrations are ~225−370 mM). We therefore hypothesize that the interactions of ^{39}K with ribosomes give rise to the large ^{39}K relaxation rates measured in the cytoplasm of *E. coli*. To test this hypothesis, we measured the transverse relaxation rates of ^{39}K (see Table 2 and Figure 4A,B) in solutions of 50S ribosomal subunits ([50S ribosome phosphate] = 119.6 mM; R_{2f} = 6.3 ± 0.6 ms^{-1} and R_{2s} = 0.47 ± 0.05 ms^{-1}) and in solutions of intact 70S ribosomal particles ([70S ribosome phosphate] = 35.5 mM; R_{2f} = 5.6 ± 0.6 ms^{-1} and R_{2s} = 0.37 ± 0.04 ms^{-1}). Cation/phosphate concentration ratios in these *in vitro* experiments were chosen to correspond most closely to those of *E. coli* samples at 1.0 OsM, where we find that R_{2f} = 5.8 ± 0.5 ms^{-1} and R_{2s} = 0.63 ± 0.06 ms^{-1}. The interactions of the ribosome with ^{39}K give rise to biexponential transverse relaxation with rates as large as those measured in viable cells and with the same large difference between R_{2f} and R_{2s}. Moreover, solutions

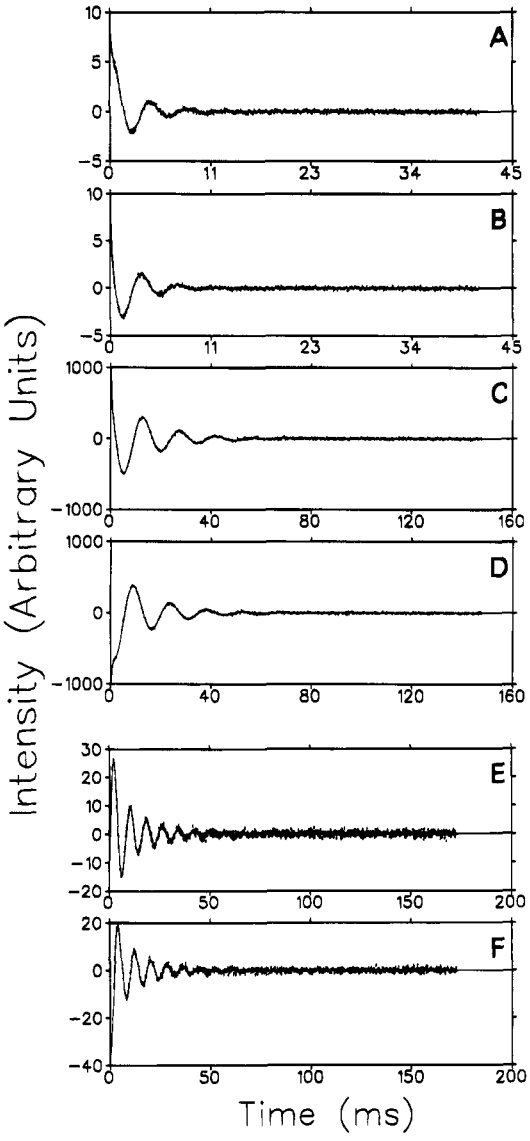

FIGURE 4: FIDs of quadrupolar ions in 70S ribosome solutions. Real and imaginary components of FIDs of ^{39}K (A, B), ^{23}Na (C, D), and ^{35}Cl (E, F) in 70S ribosome solutions. The ^{39}K FID corresponds to that reported in Table 2, footnote c. The ^{23}Na and ^{35}Cl FIDs correspond to those reported in Table 3, footnote c. The dotted lines show data and solid lines show double-exponential fittings.

that contain ribosomes, even at these low concentrations, give rise to ^{39}K transverse relaxation rates that are comparable in magnitude to those measured in viable cells, whereas ^{39}K transverse relaxation rates measured in K-DNA (0.38 ± 0.03 ms^{-1}), K-salt solutions (e.g., in KGlu, $R_2 = 0.028 \pm 0.003$ ms^{-1}), and other putatively relevant *in vitro* models for the intracellular environment of viable cells (e.g., KGlu in 470 mg/mL BSA; $R_2 = 0.099 \pm 0.003$ ms^{-1}) are not comparable (see Table 2 and Discussion).

We find the same qualitative NMR features for ^{23}Na in a ribosome solution as those found for ^{39}K in a ribosome solution (see Table 3 and Figure 4C,D). In 70S ribosome solutions, the ^{23}Na transverse relaxation is biexponential. The fast and slow ^{23}Na relaxation rates are large (e.g., $R_{2f} = 3.4 \pm 0.3$ ms^{-1} and $R_{2s} = 0.088 \pm 0.009$ ms^{-1}) and similar to those measured in viable cells (e.g., in yeast, $R_{2f} = 2.5 \pm 1.5$ ms^{-1} and $R_{2s} = 0.19 \pm 0.03$ ms^{-1}; Rooney & Springer, 1991); they also exhibit the characteristic large difference between R_{2f} and R_{2s} observed in viable cells (see below). In

Table 3: ^{23}Na Transverse Relaxation Rates

system[a]	R_2 or R_{2s}, R_{2f} (ms^{-1})	visibility (%)
yeast[d]	0.19 ± 0.03 2.5 ± 1.5	(100)
70S ribosomes[c]	0.088 ± 0.009 3.4 ± 0.3	~100[e]
70S ribosomes[f]	0.051 ± 0.005 1.5 ± 0.2	~100[e]
70S ribosomes[b]	0.070 ± 0.007 2.2 ± 0.2	not determined
Na-DNA, [P] = 7.5 mM, [Na] = 8.9 mM, [Cl] = 1.4 mM	0.070 ± 0.007 0.13 ± 0.01	100
25 mM NaCl	0.019 ± 0.003	(100)

[a] $T = 296$ K; $\omega_L = 105.845$ MHz. [b] Solution conditions are the same as the 70S ribosome sample in Table 2. [c] [ribosomal phosphate] = 44.9 mM, $[Na^+]_{total}$ = 33.8 mM, $[Cl^-]_{total}$ = 25.4 mM, $[Mg^{2+}]_{total}$ = 18.5 mM, $[NaN_3]$ = 5.0 mM, [MOPS] = 0.6 mM, and [β-mercaptoethanol] = 3 mM, pH 7.6. $[Cl^-]_{total}$ is estimated here by invoking electroneutrality and assuming that 10% of the 70S ribosomal phosphate is neutralized by positively charged ribosomal protein (Grunberg-Manago et al., 1981). [d] Rooney and Springer (1991); $T = 293$ K, ω_L = 79.38 MHz. [e] The accurate determination of amplitudes for this sample was hindered by temporary systematic fluctuations in the NMR spectrometer. However, within the error of these fluctuations (~30–40%) this signal is 100% visible. [f] Same relative concentrations as in footnote c, but pure water (conductance 18 MΩ) was added to dilute all concentrations by a factor of 8.

Table 4: ^{35}Cl Transverse Relaxation Rates

system[a]	R_2 or R_{2s}, R_{2f} (ms^{-1})	visibility (%)
70S ribosomes[c]	0.061 ± 0.006 0.28 ± 0.03	~100[e]
70S ribosomes[b]	0.064 ± 0.006 0.30 ± 0.03	not determined
Na-DNA, [P] = 7.5 mM, [Na] = 8.9 mM, [Cl] = 1.4 mM	0.030 ± 0.003	(100)[d]
4 mM NaCl	0.033 ± 0.003	(100)

[a] $T = 296$ K; $\omega_L = 39.207$ MHz. [b] Solution conditions are the same as the 70S ribosome sample in Table 2. [c] Solution conditions are the same as the 70S ribosome sample designated footnote c in Table 3. [d] We have not accurately quantified this signal. However, R_2 is equal to that in a NaCl solution, and therefore we expect that the ^{35}Cl signal in the DNA solution is in the extreme motional narrowing regime and thus 100% visible. [e] The accurate determination of amplitudes for this sample was hindered by temporary systematic fluctuations in the NMR spectrometer. However, within the error of these fluctuations (~30–40%) this signal is 100% visible.

contrast, ^{23}Na transverse relaxation rates in NaDNA solutions ($R_2 = 0.070 \pm 0.007$ ms^{-1}) or in NaCl solutions ($R_2 = 0.019 \pm 0.003$ ms^{-1}) are monoexponential.

Surprisingly, we also observe biexponential transverse relaxation for ^{35}Cl in 70S ribosome solutions (e.g., $R_{2f} = 0.28 \pm 0.03$ ms^{-1} and $R_{2s} = 0.061 \pm 0.006$ ms^{-1}; see also Table 4 and Figure 4E,F). In sharp contrast the ^{35}Cl relaxation rate in a DNA solution ($R_2 = 0.030 \pm 0.003$ ms^{-1}) is comparable to that in a NaCl solution ($R_2 = 0.033 \pm 0.003$ ms^{-1}), and therefore probably is not biexponential.

DISCUSSION

Since transverse relaxation rates of ^{23}Na and ^{39}K vary similarly as solution conditions are varied, trends and qualitative characteristics of NMR relaxation of the two nuclei *in vitro* can be considered together and compared with the behavior of ^{39}K and ^{23}Na in viable cells.

Our Measurements of ^{39}K Signals in the Cytoplasm of E. coli Are 100% Visible and Homogeneous. Many researchers have reported 40% visibility of the expected signal from spin $^3/_2$ nuclei (e.g., ^{39}K and ^{23}Na) in viable cells [reviewed by Springer (1987)]. As discussed in Materials and Methods, the loss of visibility for a spin $^3/_2$ nucleus typically occurs in the slow motional narrowing limit, where only the slower transverse relaxation rate (always 40% of the signal for a homogeneous spin $^3/_2$ signal) is detectable. The faster transverse relaxation rate (always 60% of the signal for a homogeneous spin $^3/_2$ signal) is not detected in part because of inadequate signal-to-noise and also because of the dead time required to avoid acoustic ringdown after the pulse and before acquisition of data commences in an NMR scan. A ~60% loss of signal intensity for spin $^3/_2$ NMR nuclei *in vivo* was reported previously by Ogino et al. (1983) for ^{23}Na and ^{39}K in yeast, by Shulman and collaborators for ^{23}Na in *E. coli* (Castle et al., 1986a), and by Richey et al. (1987) for ^{39}K in *E. coli*. [More recently, Rooney and Springer (1991) reported 100% NMR visibility of ^{23}Na in ^{23}Na-loaded yeast.]

The present results provide the first demonstration of 100% visibility of ^{39}K in *E. coli* which, together with the adequate fitting of the experimental FID to the biexponential functional form, demonstrates that the ^{39}K FID signal is homogeneous in the cytoplasm of *E. coli*.

The ^{39}K NMR Signal in the Cytoplasm of E. coli (without Plasmid) Does Not Exhibit Liquid Crystalline Character. The ^{39}K line shapes shown in Figure 3A,B are qualitatively consistent with those measured previously in *E. coli* (Richey et al., 1987) and in yeast (Ogino et al., 1983). Here we consider the NMR characteristics of the state (i.e., isotropic or anisotropic) of the cytoplasm as experienced by ^{39}K nuclei. ^{23}Na counterions in liquid crystalline DNA samples, at nucleic acid phosphate concentrations comparable to those in the cytoplasm of *E. coli*, exhibit up to ~400 Hz static quadrupolar splitting (i.e., separating each peak in the triplet spectrum) (Strzelecka & Rill, 1992). Edzes et al. (1972) reported quadrupolar splitting for ^{23}Na in oriented DNA fibers in the range of 1−28 kHz. We are not aware of any ^{39}K studies of liquid crystalline K-DNA systems, but the values of ^{39}K static quadrupolar splittings reported in various water−soap liquid crystalline phases are between 0 and 50 kHz (Boden & Jones, 1983; Gutman et al., 1987). These ^{23}Na and ^{39}K static quadrupolar splittings are well within the range of our sweep width. The ^{39}K spectra in Figure 3A,B show no significant static quadrupolar splitting. Further, all cell samples exhibit a simple isotropic, homogeneous spectrum and 100% visibility of the ^{39}K signal. We therefore conclude that the cytoplasm of *E. coli*, as probed by ^{39}K NMR spectroscopy, is more like an isotropic nucleic acid solution (Braunlin & Nordenskiöld, 1984) than a liquid crystalline nucleic acid array.

Using X-ray scattering, Reich et al. (1994) have observed liquid crystals of plasmid DNA in the cytoplasm of *E. coli* containing a high plasmid copy number, but no liquid crystals in cells lacking plasmid. This finding is consistent with our inference based on ^{39}K NMR that the cytoplasm is not a nucleic acid liquid crystal because our strain of *E. coli* also lacks plasmid. It will be of interest to determine whether the ^{39}K line shape in their plasmid-containing strain exhibits static quadrupolar splitting.

Relaxation Rates of Cations Measured in E. coli Are Very Fast Compared to Previous Measurements of Cation Relaxation Rates in Isotropic Solutions in Vitro. Having established that the ^{39}K NMR signal in *E. coli* is homogeneous and lacks significant static quadrupolar splitting, we now compare transverse relaxation rates measured in *E. coli* to those of putatively relevant *in vitro* biopolymer solutions in an attempt to determine the source of the large transverse relaxation rates measured in *E. coli*.

The ^{39}K relaxation rates measured in *E. coli* (and other viable cells) range from 0.61 to 1.06 ms^{-1} for R_{2s} and 5.3 to 10.0 ms^{-1} for R_{2f}. Not only are these relaxation rates large compared to all previous *in vitro* measurements of ^{39}K relaxation rates in solutions containing physiological concentrations of protein, nucleic acid and salt, but the difference between R_{2f} and R_{2s} is also very large compared to the corresponding rate constants measured *in vitro*. The large magnitude of the transverse relaxation rates and the large difference between the fast and slow relaxation rates are characteristic of quadrupolar cations in many viable cells. Recent examples of quadrupolar cation NMR relaxation rates in viable cells measured at 8.45 Tesla include ^{39}K in rat heart [$R_{2f} = 1.9$ ms^{-1} and $R_{2s} = 0.2$ ms^{-1} (Hiraishi et al., 1990)], ^{39}K in rat salivary glands [$R_{2f} = 2.5$ ms^{-1} and $R_{2s} = 0.4$ ms^{-1} (Seo et al., 1990)], ^{23}Na in yeast [$R_{2f} = 2.5$ ms^{-1} and $R_{2s} = 0.2$ ms^{-1} (Rooney & Springer, 1991)], ^{23}Na in rat salivary glands [$R_{2f} = 1.4$ ms^{-1} and $R_{2s} = 0.1$ ms^{-1} (Seo et al., 1993)], and ^{87}Rb in rat salivary gland [$R_{2f} = 9.7$ ms^{-1} and $R_{2s} = 1.7$ ms^{-1} (Steward et al., 1991)].

First we discuss data from the literature which show effects on quadrupolar cation NMR relaxation arising from the interactions of quadrupolar ions with nucleic acids under solution conditions that may be physiologically relevant. The concentration of nucleic acid in the cytoplasm of *E. coli* increases from ~260 mM nucleic acid phosphate at 0.1 OsM to ~420 mM nucleic acid phosphate at 1.0 OsM. At 0.1 OsM, the ratio of nucleic acid phosphate to potassium, $[P]/[K^+]$, is 1.5 (multivalent cations in the cytoplasm also contribute to electroneutrality); at 1.0 OsM $[P]/[K^+] = 0.77$ (Cayley et al., 1991). Measurements of ^{39}K transverse relaxation rates in K-DNA solutions, where the $[P]/[K^+]$ ratio is equivalent to that in the cytoplasm (see Background for significance of $[P]/[K^+]$), are 100% visible and are in the near-extreme motional narrowing regime (Braunlin & Nordenskiöld, 1984). At [P] = 12.3 mM, the maximum observable transverse relaxation rate of ^{39}K in a K-DNA solution under "salt-free" conditions, where $[P]/[M^+] = 1.0$, is ~0.75 ms^{-1} [extrapolated from the data of Braunlin and Nordenskiöld (1984)]. Measurements of ^{23}Na in concentrated isotropic phase mononucleosomal DNA solutions always are in the near-extreme motional narrowing regime at 40.04 MHz and have relaxation rates that are small compared to those measured in viable cells (Strzelecka, 1988; Strzelecka & Rill, 1990; Strzelecka & Rill, 1992). For example, a solution containing 170 mg/mL DNA (0.52 M DNA phosphate) at 0.53 M Na^+ exhibits a transverse relaxation rate of 0.19 ms^{-1} in the near-extreme motional narrowing regime. On the other hand, the ^{23}Na transverse relaxation rates in *E. coli* and yeast (measured at higher frequencies where lower relaxation rates are expected) are in the slow motional narrowing regime with R_{2f} ~2.5 ms^{-1} [Rooney and Springer (1991) at 79 MHz] and R_{2s} ~0.2−0.4 ms^{-1} [Castle et al. (1987) at 95 MHz; Rooney and Springer (1991) at 79 MHz]. Thus, isotropic DNA solutions exhibit cation transverse relaxation rates significantly smaller

than those measured in *E. coli* or yeast.

James and Noggle (1969a,b) reported 100% signal visibility, a single exponential transverse relaxation and $R_1 = \sim 0.16\ ms^{-1}$ in a solution of 20 mg/mL soluble yeast RNA (a sample primarily of transfer RNA) and 50 mM NaCl at a ^{23}Na resonance frequency of 15 MHz. Because of the very low field strength used in these early experiments and the fact that relaxation rates decrease with increasing field strength, this moderately large magnitude for the longitudinal relaxation rate is not directly comparable to ^{23}Na longitudinal relaxation rates that were measured subsequently in solutions of yeast (Rooney & Springer, 1991). Since Rooney and Springer (1991) measured R_{2f}, R_{2s}, and R_1 at 79 MHz, we can estimate an absolute lower limit of R_1 for ^{23}Na at 15 MHz in yeast (cf. Appendix). Using the value of the spectral density function at 79 MHz [i.e., $J(79\ MHz)$] predicted from ^{23}Na relaxation rates (R_{2f}, R_{2s}, and R_1) measured in yeast (Rooney & Springer, 1991) as a lower estimate for both $J(15$ MHz) and $J(30$ MHz), we obtain an absolute lower bound of $R_1 \gtrsim 0.3$ ms of ^{23}Na in yeast (by assuming the near-extreme motional narrowing approximation for R_1; Bull, 1972; Halle & Wennerström, 1981). Thus, the longitudinal relaxation rates of ^{23}Na in solutions of soluble yeast RNA are substantially smaller (at least 2-fold) than those measured in yeast solutions.

Since the total cytoplasmic protein concentration in *E. coli* increases from ~200 mg/mL at 0.1 OsM to 320 mg/mL at 1.0 OsM (Cayley et al., 1991), we examine the effects of protein concentration in this general concentration range on cation NMR relaxation rates. Typically, cation quadrupolar NMR relaxation rates measured in solutions of moderately high concentration of neutral protein are slightly dependent on protein concentration but are always small compared to ^{39}K transverse relaxation rates in *E. coli* and DNA solutions *in vitro*. For example, in a 450 mg/mL BSA solution with 0.75 M KGlu, we observe 100% visibility and a transverse relaxation rate of ^{39}K of $0.163\ ms^{-1}$. Also, Ogino et al. (1985) measured ^{39}K $R_2 \sim 0.16\ ms^{-1}$ and for ^{23}Na $R_2 \sim 0.23\ ms^{-1}$ in human erythrocytes (~300 mg/mL hemoglobin), and Shinar and Navon (1984) measured the ^{23}Na transverse relaxation rate to be $\sim 0.19\ ms^{-1}$ in a solution containing 0.1 M NaCl and ~200 mg/mL hemoglobin. ^{23}Na and ^{39}K in BSA and Hb solutions and in red blood cells are all 100% visible in the near-extreme motional narrowing regime, and the relaxation rates are small compared to those measured in viable cells (Ogino et al., 1985; Shinar & Nivon, 1984).

Seo et al. (1993) and Pekar and Leigh (1986) report ^{23}Na transverse relaxation rates in the slow motional narrowing regime in solutions containing high concentrations of BSA (~580 and ~550 mg/mL, respectively) with high concentrations of NaCl (~1.7 and ~2.0 M, respectively). These relaxation rates [$R_{2f} = 0.44\ ms^{-1}$ and $R_{2s} = 0.13\ ms^{-1}$ (Seo et al., 1993); $R_{2f} = 1.3\ ms^{-1}$ and $R_{2s} = 0.3\ ms^{-1}$ (Pekar and Leigh, 1986)] are larger than in most systems *in vitro*. However, these two BSA solutions contain higher concentrations of protein and salt, and a far lower concentration of free water, than the range investigated in *E. coli* and yeast. The total *E. coli* cytoplasmic macromolecular concentration is between 275 and 475 mg/mL, and the *E. coli* cytoplasmic molar potassium concentration is between 0.17 and 0.55 M (Cayley et al., 1991). The cytosol of yeast has a macromolecular concentration on the order of 20% w/w (~210 mg/mL) (Fulton, 1982). Although the magnitudes of the ^{23}Na relaxation rates in these two BSA solutions are comparable to those measured in some viable cells, the difference between R_{2f} and R_{2s} is small compared to that typically observed in viable cells. It is possible that the large relaxation rates seen in these two BSA solutions result from the depletion of a bulk water phase. Indeed, these results may be useful in understanding the behavior in plasmolyzed cells reported here (see below).

Solutions containing moderately high concentrations (between 350 and 450 mg/mL) of highly charged proteins are observed to have transverse relaxation rates that are large and in the slow motional narrowing regime [e.g., ^{23}Na and ^{39}K in eye lens extracts (Stevens et al., 1992) and ^{39}K in BSA with added KOH to increase the net charge on BSA (H.J.G., M.L., and M.T.R., unpublished results)] but are not as large as the relaxation rates in yeast or *E. coli*. The relevance of these NMR relaxation rate studies to the NMR properties of quadrupolar cations in *E. coli* may be questioned because the net charge on the average cytoplasmic protein in *E. coli* is expected to be positive and small (<+2; Cayley et al., 1991). Nevertheless, detailed study of quadrupolar relaxation of cations in well-characterized solutions of charged protein may be a useful avenue for understanding quadrupolar relaxation in ribosome solutions.

We also examined the possible effects of cytoplasmic viscosity on the ^{39}K transverse relaxation. The cytoplasmic viscosity of *E. coli*, as reported by the ^{13}C NMR determined rotational correlation time of trehalose (a cytoplasmic disaccharide), is approximately a factor of 1.5 greater than that of pure water, comparable to a solution containing 0.3 M trehalose (Lewis et al., 1990). In a solution containing 0.4 M sucrose and 1 M KCl we measure a ^{39}K transverse relaxation rate of $0.05\ ms^{-1}$, only slightly larger than that in 1 M KCl. Therefore effects due to increased viscosity are by themselves insufficient to explain the large ^{39}K transverse relaxation rates that are observed in the cytoplasm of *E. coli*.

Ribosomes in Vitro and in Viable Cells Produce the Same Distinctive Characteristics of ^{39}K and of ^{23}Na NMR Relaxation. ^{39}K and ^{23}Na NMR relaxation rates in ribosome solutions are much larger than those in DNA or in salt solutions and are comparable to those measured in the cytoplasm of *E. coli* and in yeast (see Tables 2 and 3). We propose that NMR relaxation rates of these cations observed in *E. coli* and yeast are also dominated by the presence of ribosome particles in the cytoplasm and in the cytosol, respectively.

The biexponential behavior of the ^{35}Cl transverse relaxation in ribosome solutions is very surprising in view of the fact that the ribosome has a net negative charge of ~4500 (Goldberg, 1966; Grunberg-Manago et al., 1981) and therefore should exclude ^{35}Cl from its vicinity by coulombic repulsion. Biexponential behavior is observed in systems where ^{35}Cl binds to proteins (Shacher-Hill & Shulman, 1992; Xu et al., 1989). Since ribosomes do contain highly positively charged proteins (Goldberg, 1966), we considered the possibility that chloride may bind to ribosome proteins. We find that a 50-fold increase in Cl^- concentration (from 10 to ~500 mM, by addition of $MgCl_2$ and NaCl to the ribosome solution) yields a ^{35}Cl transverse relaxation that remains in the slow motional narrowing regime with transverse relaxation rates reduced by only ~10%. In contrast, a 50-fold increase in Cl^- concentration (from 10 to ~500 mM) in a 150 mg/mL solution of dromedary

hemoglobin (shown, by ^{35}Cl NMR, to have two binding sites for ^{35}Cl) reduces the transverse relaxation rates by a factor of ~5 (Lundberg et al., 1989).

Whereas it appears that ^{23}Na and ^{39}K NMR relaxation in the cytoplasm of *E. coli* are dominated by the presence of ribosome subunits or particles, ^{35}Cl NMR relaxation may not be dominated by this interaction. For example, when the membranes of *E. coli* are partially permeabilized by toluene in the presence of a ^{35}Cl shift reagent, the visibility of the shifted (i.e., extracellular) ^{35}Cl NMR signal decreases without the appearance of an unshifted (i.e., intracellular) ^{35}Cl signal (Shachar-Hill & Shulman, 1992). This decrease in total visibility implies that ^{35}Cl is leaking into the cells and that the intracellular ^{35}Cl is 100% invisible. Therefore, the ^{35}Cl signal in the cytoplasm may be dominated by the interaction of ^{35}Cl with proteins even though the relaxation rates are also increased by the presence of ribosomes. Indeed, ^{35}Cl NMR relaxation rates are increased in the presence of proteins (Forsén & Lindman, 1981) and are very fast at low concentrations of the anion-binding protein BSA (i.e., ~24 mg/mL; Shachar-Hill & Shulman, 1992).

We propose that all ribosome-containing cells will exhibit similar large relaxation rate enhancements for cytoplasmic quadrupolar nuclei if the quadrupolar nucleus experiences the ribosomal particle *in vivo*. Indeed, *E. coli* (Castle et al., 1986a; Richey et al., 1987), yeast (Ogino et al., 1983; Rooney & Springer, 1991), halobacteria (Shporer & Civan, 1977), rat heart (Hiraishi et al., 1990), and rat salivary glands (Seo et al., 1990, 1993; Steward et al., 1991) all show enhanced cation quadrupolar relaxation rates. On the other hand, red blood cells and nucleated red blood cells (Shinar & Navon, 1991) (which presumably do not contain ribosomes, but do contain nuclei, with [DNA] = ~20 mg/mL and [Hb] = ~300 mg/mL) exhibit neither these large ^{23}Na transverse relaxation rates nor the characteristic large difference between R_{2f} and R_{2s}.

Plasmolyzed Cells Show a Large Increase in the Transverse Relaxation Rates of ^{39}K. The plasmolyzed cell slurries show large increases in the ^{39}K transverse relaxation rates compared to any of the other cell samples. The plasmolyzed cells have the same relative concentrations as those of cells grown at 0.1 OsM, but since the volume of the cytoplasm is reduced by a factor of 3 upon plasmolysis (Cayley et al., 1991), the absolute concentrations of all molecular species in the cytoplasm are higher by a factor of 3 in the plasmolyzed cells. It is very possible that the increased ribosome concentration in the plasmolyzed cells increases significantly the transverse relaxation rate of ^{39}K measured in cell slurries, because our measurements show a large dependence on ribosome concentration of the NMR relaxation rates of quadrupolar ions (^{23}Na, ^{39}K, and ^{35}Cl) in ribosome solutions. For example, 8-fold dilution of a ribosome solution with water causes the ^{23}Na relaxation rates to decrease by a factor of ~2 (see Table 3). We have observed this dependence for ^{23}Na, ^{39}K, and ^{35}Cl in the concentration range of 10 μM to 35 mM [P] in solutions containing 70S particles. We are continuing to examine the physical basis of the ribosome concentration dependence of the NMR relaxation rates of ^{39}K, ^{23}Na, and ^{35}Cl.

The dependence of cation transverse relaxation rates on the ribosomal nucleic acid concentration between 10 μM and 35 mM [P] contrasts with that seen in DNA solutions. Van Dijk et al. (1987) reported very little, if any, dependence of ^{23}Na R_1, R_{2s}, and R_{2f} on [P] when measured in a DNA solution which had [P]/[Na] = 1.0 and the DNA phosphate concentrations were varied from 1 mM [P] to 0.1 M [P]. However, at DNA phosphate concentrations larger than 0.5 M, ^{23}Na transverse relaxation rates may be dependent on DNA phosphate concentration. Data collected by Strzelecka and Rill (Strzelecka, 1988; Strzelecka & Rill, 1990, 1992) indicate some dependence of ^{23}Na R_2 (R_2 in the near-extreme motional narrowing regime at 40.04 MHz at all isotropic solution conditions in their experiments) on DNA phosphate concentration since $R_2 = 0.19$ ms^{-1} both in a solution where [P]/[Na] = 0.98 and [P] = 0.52 M and in a solution where [P]/[Na] = 0.42 and [P] = 0.73 M. (If there were no dependence on [P], then R_2 would decrease with decreasing [P]/[Na].) Also, effects due to the large salt concentration typically are not significant unless macromolecular concentrations exceed 400 mg/mL. Thus, the observation that R_2 remains unchanged while [P]/[Na] is decreased by a factor of 2.4 implies that an increase in [P] concentration at constant [P]/[Na] would cause the ^{23}Na transverse relaxation rate to increase significantly.

Dehydration is a factor which may contribute to the large transverse relaxation rates in plasmolyzed cells. Dehydration, or the loss of bulk cytoplasmic water (which decreases the cytoplasmic volume), is caused by the high external osmolarity of the plasmolyzing media in conjunction with only permitting the cells to respond by loss of water [see Cayley et al. (1991)]. For unplasmolyzed cells grown at 0.1 OsM we estimate that there is ~1 hydration (nonbulk) water for every 5 bulk water molecules (Cayley et al., 1991). However, for the plasmolyzed cells we estimate that there is >1 hydration water for every bulk water molecule (Cayley et al., 1991). Previous studies of concentrated BSA solutions with high concentrations of NaCl [[BSA] = ~580 mg/mL, ~1.7 M NaCl, $R_{2f} = 0.44$ ms^{-1}, $R_{2s} = 0.13$ ms^{-1} (Seo et al., 1993); [BSA] = 50% w/w, ~2.0 M NaCl, $R_{2f} = 1.3$ ms^{-1}, $R_{2s} = 0.3$ ms^{-1} (Pekar & Leigh, 1986)] show large ^{23}Na transverse relaxation rates in the slow motional narrowing regime. In a high-salt solution of 540 mg/mL of BSA (~48% w/w) with 1.5 M NaCl in 100% H_2O, we find that the ^{23}Na transverse relaxation is in the slow motional narrowing regime ($R_{2f} = 0.34$ ms^{-1}, $R_{2s} = 0.094$ ms^{-1}). However, in a low-salt solution containing 530 mg/mL of BSA but only 1 mM [NaCl] in 100% H_2O, the ^{23}Na transverse relaxation rates are $R_{2f} = 0.14$ ms^{-1} and $R_{2s} = 0.072$ ms^{-1}. Since a solution of 1.5 M NaCl without BSA does not have a large R_2 and the ^{23}Na NMR relaxation rates decrease when [NaCl] is reduced in a 500 mg/mL BSA solution, the large ^{23}Na NMR relaxation rates are probably a result of dehydration. Thus, the loss of bulk water can lead to significant increases in the NMR relaxation rates of quadrupolar ions. We therefore propose that dehydration may also contribute to the large ^{39}K transverse relaxation rates we measure in plasmolyzed cell slurries.

Since the viscosity (as reported by ^{13}C NMR correlation times of 10 mM glycine) in a 500 mg/mL BSA solution is only a factor of ~2.4 greater than that of pure water (Endre & Kuchel, 1986), the increase in microscopic viscosity is probably not responsible for the large relaxation rates measured in these BSA solutions. Indeed, our measurements of ^{39}K in trehalose (see above) show that this small increase in viscosity does not lead to a significant increase in the ^{39}K relaxation rate.

The Contributions to the NMR Relaxation Rates of Quadrupolar Cations in Viable Cells. By comparison of the distributions of correlation times, Rooney and Springer (1991) have suggested that a 550 mg/mL BSA solution with 1.4 M NaCl in 100% D_2O is an appropriate NMR model to describe ^{23}Na NMR in yeast. However, both this macromolecular concentration and salt concentration are much larger than those typical of the cytosol of yeast (Fulton, 1982). Hence a concentrated BSA solution at high salt is probably not an appropriate model for the cytoplasm of a viable cell. In addition, Rooney and Springer find that R_{2f} in the BSA solution and in yeast are different by a factor of 3, and that the difference between R_{2f} and R_{2s} in BSA ($R_{2f} - R_{2s} = 0.6$ ms^{-1}) is much smaller than that in yeast ($R_{2f} - R_{2s} = 2.3$ ms^{-1}). We propose that the large values of the ^{23}Na relaxation rates observed in their BSA solution can be explained by dehydration (as described above) and that the interaction of Na with ribosomes in yeast (and in all viable cells) is the dominant effect on ^{23}Na NMR relaxation.

We propose on the basis of our *in vivo* and *in vitro* experiments, and the above cited work of other laboratories, that at least three factors contribute to the ^{39}K NMR behavior as a function of osmolarity of growth and plasmolysis in the cytoplasm of *E. coli*. The dominant effect upon increasing the external osmolarity on ^{39}K NMR relaxation is the accumulation of potassium and hence the decrease in the ratio [P]/[K$^+$]. The *in vitro* study of ^{39}K NMR in the presence of DNA (Braunlin & Nordenskiöld, 1984) indicates that this decrease in [P]/[K$^+$] would cause a drastic reduction in the relaxation rates of ^{39}K in the cytoplasm as the external osmolarity is increased (a decrease in [P]/[K$^+$] caused by addition of K$^+$ is expected to increase the fraction of "free" ^{39}K not affected by nucleic acid—see also the comments on the two state model in the NMR Background section). Secondly, increasing the external osmolarity reduces the amount of cytoplasmic water and therefore increases the ribosome concentration. We observe an increase in the quadrupolar relaxation of ions when the ribosome concentration is increased. We propose that the reduction in [P]/[K$^+$] and the increase in ribosome concentration with increasing osmolarity of growth have partially compensating effects on the ^{39}K relaxation rates we measured in *E. coli* cell slurries. Loss of bulk water may also contribute to the increase in ^{39}K NMR transverse relaxation rate in growing cells as the osmolarity is increased, but this effect on the ^{39}K transverse relaxation is probably smaller than the first two effects.

CONCLUSIONS

In general, the relaxation rates of quadrupolar cations in viable cells (a) are in the slow motional narrowing regime, (b) have very fast relaxation rates compared to simple salt solutions, and (c) exhibit very large differences between the fast and slow relaxation rates. We show for the first time that *in vitro* measurements of ^{23}Na and ^{39}K in solutions containing ribosomes have all three of these characteristics. In contrast, our novel analysis shows that ^{39}K and ^{23}Na transverse relaxation in concentrated macromolecular solutions consisting individually of proteins, DNA, and soluble RNA do not exhibit all of these three characteristics. We propose that all cells containing ribosomes, where quadrupolar cations interact with the ribosomes, will show these three characteristics. In addition, we report for the first time 100% visibility of ^{39}K NMR signals in concentrated *E. coli* cell slurries. We find that the cytoplasm of *E. coli* as experienced by ^{39}K NMR is more like an isotropic nucleic acid solution, rather than a nucleic acid liquid crystal. We propose that the lack of a strong dependence of ^{39}K relaxation rates in *E. coli* cell slurries on osmolarity of the growth medium is a result of two largely compensating effects. As the osmolarity of the growth media increases, the concentration of ribosomal phosphate tends to cause an increase in the ^{39}K relaxation rates, while the increase in [K$^+$]/[P] tends to cause a decrease in the ^{39}K relaxation rates. Finally, we propose that the large increase in the relaxation rates of the plasmolyzed cells compared to the unplasmolyzed cells can be explained qualitatively by the increase in the ribosomal phosphate concentration but may also have a significant contribution due to dehydration (i.e., loss of bulk water).

ACKNOWLEDGMENTS

We thank Drs. Peter Moore and Betty Freeborn for the generous gift of large quantities of 50S and 70S ribosomes and for discussions concerning ribosome purification. We thank Dr. Veronica Stein for providing us with the DNA sample, Dr. Matt Sanders for his help and discussions concerning the use of the ICPES and the flame emission spectrometer, Dr. Mark Anderson for helpful discussions on NMR instrumentation and for modifying a pre-amp match unit to the ^{39}K frequency, Dr. Fritz Abildgaard for general NMR instrumentation help and useful discussions concerning data format of Bruker data files, Jane Caldwell for help with FELIX, and Dr. Charles Springer for comments on the manuscript. This study made use of the National Magnetic Resonance Facility at Madison, which is supported by NIH from the Biomedical Research Technology Program, National Center for Research Resources. Equipment in the facility was purchased with funds from the University of Wisconsin, the NSF Biological Instrumentation Program, NIH Biomedical Research Technology Program, NIH Shared Instrumentation Program, and the U.S. Department of Agriculture. We are pleased to acknowledge Dr. John Markley and his staff for providing access to and support of this superb instrumentation.

APPENDIX

Obtaining the Spectral Densities $J(0)$, $J(\omega_L)$, and $J(2\omega_L)$ from R_{2f}, R_{2s}, and R_1. Obtaining the values of the spectral densities directly from the relaxation rates is important because the values of the spectral densities so obtained are model-independent if the signal is homogeneous and in the motional narrowing regime. For a nucleus with spin = $^3/_2$ where the transverse relaxation is in the slow motional narrowing regime and the longitudinal relaxation is in the near-extreme motional narrowing regime, we obtain (Halle & Wennerström, 1981; Hubbard, 1970; Tromp et al., 1991)

$$R_{2f} = J(0) + J(\omega_L)$$

$$R_{2s} = J(\omega_L) + J(2\omega_L)$$

$$R_1 = 0.4J(\omega_L) + 1.6J(2\omega_L)$$

Rearrangement then gives

$$J(2\omega_L) = (5R_1 - 2R_{2s})/6$$

$$J(\omega_L) = (8R_{2s} - 5R_1)/6 = R_{2s} - J(2\omega_L)$$

$$J(0) = R_{2f} - J(\omega_L)$$

Thus, if R_{2f}, R_{2s}, and R_1 are measured $J(2\omega_L)$, $J(\omega_L)$, and $J(0)$ can be calculated for a homogeneous signal in the motional narrowing regime.

REFERENCES

Anderson, C. F., & Record, M. T., Jr. (1990) *Annu. Rev. Biophys. Biophys. Chem. 19,* 423−465.

Boden, N., & Jones, S. A. (1983) *Isr. J. Chem. 23,* 356−362.

Braunlin, W. H., & Nordenskiöld, L. (1984) *Eur. J. Biochem. 142,* 133−137.

Bull, T. E. (1972) *J. Magn. Reson. 8,* 344−353.

Castle, A. M., Macnab, R. M., & Shulman, R. G. (1986a) *J. Biol. Chem. 261,* 3288−3294.

Castle, A. M., Macnab, R. M., & Shulman, R. G. (1986b) *J. Biol. Chem. 261,* 7797−7806.

Cayley S., Record M. T., Jr., & Lewis B. A. (1989) *J. Bacteriol. 171,* 3597−3602.

Cayley S., Lewis B. A., Guttman H. J., & Record M. T., Jr. (1991) *J. Mol. Biol. 222,* 281−300.

Edzes, H. T., Rupprecht, A., & Berendsen, H. J. C. (1972) *Biochem. Biophys. Res. Commun. 46,* 790−794.

Endre, Z. H., & Kuchel, P. W. (1986) *Biophys. Chem. 24,* 337−356.

Forsén, S., & Lindman, B. (1981) *Methods Biochem. Anal. 27,* 289−486.

Fouques, C. E. M., & Werbelow, L. G. (1979) *Can. J. Chem. 57,* 2329−2332.

Foy, B., D., & Burstein, D. (1990) *Biophys. J. 58,* 127−134.

Fulton, A. B. (1982) *Cell 30,* 345−347.

Fushima, E., & Roeder, S. B. W. (1981) *Experimental Pulse NMR: A Nuts and Bolts Appoach,* pp 218−227, Addison-Wesley Publishing Company, Redwood City, CA.

Goldberg, A. (1966) *J. Mol. Biol. 15,* 663−673.

Grunberg-Manago, M., Hut Bon Hoa, G., Douzou, P., & Wishnia, A. (1981) in *Metal Ions in Genetic Information Transfer* (Eichhorn, G. L., & Marzilli, L. G., Eds.) pp 191−232, Elsevier North Holland, New York.

Gutman, H., Luz, Z., Charvolin, J., & Loewestein, A. (1987) *Liq. Crys. 2,* 739−755.

Halle, B., & Wennerström, H. (1981) *J. Magn. Reson. 44,* 89−100.

Hirasihi, T., Seo, Y., Murakami, M., & Watari, H. (1990) *J. Magn. Reson. 87,* 169−173.

Hubbard, P. S. (1970) *J. Chem. Phys. 53,* 985−987.

James, T. L., & Noggle J. H. (1969a) *Proc. Natl. Acad. Sci. U.S.A. 62,* 644−649.

James, T. L., & Noggle J. H. (1969b) *J. Am. Chem. Soc. 91,* 3424−3428.

Johnson, M. L., & Frasier S. G. (1985) *Methods Enzymol. 117,* 301−342.

Lewis, B. A., Cayley, S., Padmanabhan, S., Kolb, V. M., Brushaber, V., Anderson, C. F., & Record, M. T., Jr. (1990) *J. Magn. Reson. 90,* 612−617.

Lundberg, P., Vogel, H., Drakenberg, T., Forsén, S., Amiconi, G., Forlani, L., & Chiancone, E. (1989) *Biochim. Biophys. Acta 999,* 12−18.

Noelken, M. E., & Timasheff, S. N. (1967) *J. Biol. Chem. 242,* 5080−5085.

Ogino, T., den Hollander, J. A., & Shulman, R. G. (1983) *Proc. Natl. Acad. Sci. U.S.A. 80,* 5185−5189.

Ogino, T., Shulman, G. I., Gullans, S. R., den Hollander, J. A., & Shulman, R. G. (1985) *Proc. Natl. Acad. Sci. U.S.A. 82,* 1099−1103.

Pekar, J., & Leigh, J. S., Jr. (1986) *J. Magn. Reson. 69,* 582−584.

Reich, Z., Wachtel, E. J., & Minsky, A. (1994) *Science 264,* 1460−1463.

Richey, B. R., Cayley, D. S., Mossing, M. C., Kolka, C., Anderson, C. F., Farrar, T. C., & Record, M. T., Jr. (1987) *J. Biol. Chem. 262,* 7157−7164.

Rooney, W. D., & Springer, C. S., Jr. (1991) *NMR Biomed. 4,* 227−245.

Rooney, W. D., Barbara, T. M., & Springer, C. S., Jr. (1988) *J. Am. Chem. Soc. 110,* 674−681.

Seo, Y., Murakami, M., Suzuki, E., Kuki, S., Magayama, K., & Watari, H. (1990) *Biochemistry 29,* 599−603.

Seo, Y., Rooney, W. D., & Murakami, M. (1993) *Biochim. Biophys. Acta 1177,* 111−116.

Shachar-Hill, Y., & Shulman, R. G., (1992) *Biochemistry 31,* 6272−6278.

Shporer, M., & Civan, M. M. (1977) *J. Membr. Biol. 33,* 385−400.

Shinar, H., & Nivon G. (1984) *Biophys. Chem. 20,* 275−283.

Shinar, H., & Nivon G. (1991) *Biophys. J. 59,* 203−208.

Springer, C. S., Jr. (1987) *Annu. Rev. Biophys. Biophys. Chem. 16,* 375−399.

Stein, V. M., Bond, J. P., Capp, M. W., Anderson, C. F., Record, M. T., Jr. (1995) *Biophys. J.* (in press).

Stevens, A., Paschalis, P., & Schleich, T. (1992) *Biophys. J. 61,* 1061−1075.

Steward, M. C., Seo, Y., Murakami, M., & Watari, H. (1991) *Proc. R. Soc. London B 243,* 115−120.

Straume, M., Fraisier-Cardoret, S. G., & Johnson, M. L. (1991) in *Topics of Fluorescence Spectroscopy, Vol. 2: Principles* (Lakowicz, J. P., Ed.) pp 177−240, Plenum Press, New York.

Strzelecka, T. E. (1988) Thesis, Florida State University.

Strzelecka, T. E., & Rill, R. L. (1990) *Biopolymers 30,* 803−814.

Strzelecka, T. E., & Rill, R. L. (1992) *J. Chem. Phys. 96,* 7796−7807.

Tromp, R. H., van der Maarel, J. R. C., de Bleijser, J., & Leyte, J. C. (1991) *Biophys. Chem. 41,* 81−100.

Werbelow, L. G. (1979) *J. Phys. Chem. 12,* 5381−5383.

Werbelow, L. G., & Marshall, A. G. (1981) *J. Magn. Reson. 43,* 443−448.

van Dijk, L., Gruwel, M. L. H., Jesse, W., de Bleijser, J., & Leyte, J. C. (1987) *Biopolymers 26,* 261−284.

Wishnia, A., Boussert, A., Graffe, M., Dessen, Ph., & Grunberg-Manago, M. (1975) *J. Mol. Biol. 93,* 499−515.

Xu, Y., Barbara, T. M., Rooney, W. D., & Springer, C. S., Jr. (1989) *J. Magn. Reson. 83,* 279−298.

BI942313A